

# Using pedotransfer functions to improve the precision of spatially predicted available water capacity

**J. M. Austin<sup>a</sup>, U. Stockmann<sup>b</sup> and K. Verburg<sup>b</sup>**

<sup>a</sup> CSIRO Land and Water, Canberra, <sup>b</sup> CSIRO Agriculture and Food, Canberra  
Email: [jenet.austin@csiro.au](mailto:jenet.austin@csiro.au)

**Abstract:** Knowledge about soil water is critical for dryland agriculture. The amount of plant available water (PAW) is important for crop management decisions such as whether to sow or not, choice of crop or variety and addition of fertilizer. Understanding the variation of the available water capacity (AWC) of soil through the landscape can be achieved by using spatial modelling techniques such as Digital Soil Mapping (DSM). DSM predictions of AWC can be done outright using point data from field sites or with pedotransfer functions (PTFs) that use other modelled soil attributes as inputs. DSM methods allow for the inclusion of the prediction uncertainties associated with modelled datasets. One technique to account for these uncertainties is to use Latin Hypercube sampling in PTF predictions to generate multiple bounded realisations of the input data.

The Soil and Landscape Grid of Australia (SLGA) provides AWC as a soil attribute that was produced using depth-harmonized point data and formal DSM methods. The aim of this paper was to test whether AWC can be modelled with greater precision by using the more reliably-predicted soil attributes such as clay and sand percentage as input parameters to PTFs. The evaluation was over the six standard *GlobalSoilMap* depths.

To evaluate the precision of the modelled AWC datasets, the SLGA AWC mean value, 90% Prediction Interval (90% PI) and (for the 0-1 m depth aggregation) standard deviation datasets were compared with three PTF-derived AWC predictions across a study area covering the grain growing regions of Queensland and NSW. The differences in each grid cell were averaged across the study area and then normalised by the thickness of the depth layer.

The general trend for all three PTF-derived AWC datasets is to predict smaller mean AWC values than the SLGA AWC for the study area, albeit with some differences between them. In all cases the predictions had greater precision than the SLGA AWC. That is, the 90% PI is smaller for the PTF-derived AWC datasets compared to the SLGA AWC, and this difference is consistent going down the soil profile to 1 m.

The results presented here show that it is likely that modelling AWC using PTFs will give a more precise prediction of AWC than the methods attempting to predict AWC outright, like those which produced the SLGA AWC. One reason for this is that there is limited field-measured point data available to use when modelling AWC directly. Further work will include an assessment of PTF uncertainty and validation of PTF outputs against field-measured AWC to assess the accuracy of the predictions.

**Keywords:** *Digital soil mapping, pedotransfer function, uncertainty, (plant) available water capacity*

## 1. INTRODUCTION

Soil water is often critical for dryland agricultural production. Information about the amount of soil water available to crops, the plant available water (PAW), is an important factor in crop management decisions. The PAW can inform whether to sow or not, the crop and variety chosen, and various other management decisions such as the amount of fertilizer to add (Verburg et al. 2017). The amount of PAW can be estimated from the amount of water a soil can hold, the plant available water capacity (PAWC), and the soil's current volumetric water content. The PAWC of a soil is calculated for a specific crop as the difference between the Drained Upper Limit of a soil (DUL; the amount of water a soil can hold against gravity, also referred to as field capacity) and the Crop Lower Limit (CLL; the amount of water the crop can extract from a soil). When CLL data are unavailable, the 15-bar water content (LL15; a laboratory-derived soil water content when soil is under pressure of -15 bar) is often used to calculate a non-crop specific available water capacity (AWC) which assumes full root exploration.

The (P)AWC is dependent on soil physical and chemical properties, with soil texture being one of the main factors. In turn, the soil's characteristics are affected by parent material, topography, organisms, climate and time (Jenny 1941). Assessment of soil characteristics in the context of agricultural resource assessment has led to a variety of field surveys, soil classifications and mapping of soil attributes. In the last twenty years, digital soil mapping (DSM; McBratney et al. 2003) methods have become widely used for estimating soil properties over large areas and whole continents, including for estimating (P)AWC. The soil properties, referred to from here as attributes, can be predicted outright using point data from field sites or with pedotransfer functions (PTFs) that use other modelled soil attributes as inputs. The PTFs use easy to measure basic soil physical attributes such as sand content, clay content and bulk density (BD), and soil chemical attributes such as soil organic carbon (OC) content and cation exchange capacity (CEC), to estimate attributes that are more difficult to measure in the field (Bouma 1989).

As DSM methods have evolved, the focus has shifted to using the prediction uncertainties of soil attributes to assess precision and applicability. When using modelled soil attributes as inputs to other models, incorporating the known variance and uncertainties of these datasets instead of assuming these are error free can help to improve the reliability assessment of model outputs (e.g. Malone et al. 2015). One approach to efficiently incorporate prediction uncertainties, rather than simple random sampling, is to use Latin Hypercube (LHC; Pebesma and Heuvelink 1999) sampling to generate tens to thousands of realisations of the input variables before running a model. LHC sampling allows the user to understand the magnitude and effect that uncertainties contribute to downstream analyses. Additionally, the LHC sampling can include a correlation matrix of the input variables, thereby producing sensible realisations of each input. The multiple output realisations produced by a model can then be assessed for precision and accuracy.

Soil attribute layers have been produced from point data using formal DSM methods at a spatial resolution of 3 arcseconds for Australia and made publicly available as the National Soil Attribute Maps in the Soil and Landscape Grid of Australia (SLGA; Grundy et al. 2015, Viscarra Rossel et al. 2015). The DSM model for the SLGA AWC output only explained ~30% of the total variation present whereas other soil attribute models explained up to ~80% (Viscarra Rossel et al. 2015). This is linked to the considerably smaller number of points with DUL and CLL field data available for the outright prediction of AWC compared to other soil attributes in the SLGA suite. In this paper, our aim is to test whether AWC can be modelled more precisely using PTFs with the more reliably-predicted SLGA soil attributes as input parameters. To do this, we compared the uncertainties of three PTF-derived AWC datasets with the published SLGA AWC dataset (Viscarra Rossel et al. 2014), using LHC sampling and correlation matrices to incorporate input variable uncertainty within the PTF modelling.

## 2. METHOD

### 2.1. Study Area

The focus area for this work is the Grains Research and Development Corporation's (GRDC) Northern Region which covers the grain growing regions of Queensland and NSW (Figure 1).

### 2.2. Data

#### *Input Variables*

The input datasets used in the PTF modelling are soil attributes from the SLGA (Grundy et al. 2015; Viscarra Rossel et al. 2014; Viscarra Rossel et al. 2015), specifically Clay (%), Sand (%), Bulk Density (BD; g cm<sup>-3</sup>),

Organic Carbon (OC; %), Effective Cation Exchange Capacity (CEC; meq / 100g) and Depth of Soil (DES; m). The Estimated Value (mean) and the confidence interval limits (5<sup>th</sup> and 95<sup>th</sup> percentile) layers were downloaded for all six of the *GlobalSoilMap* depths (0-5 cm, 5-15 cm, 15-30 cm, 30-60 cm, 60-100 cm and 100-200 cm). These datasets and their metadata are available from <https://data.csiro.au/collections/> and <http://www.clw.csiro.au/aclep/soilandlandscapegrid/ProductDetails-SoilAttributes.html>.



**Figure 1.** Study area location within Australia shown in grey

### **Comparison AWC Dataset**

The comparison dataset for this work is the existing SLGA AWC product which is described in Viscarra Rossel et al. (2015). The SLGA soil attribute prediction method used historical soil site data and visible and infrared soil site spectra harmonized to the six *GlobalSoilMap* depths. This harmonized site data was incorporated with more than 30 environmental variables in a modelling procedure that included bootstrap sampling, a decision tree and piecewise regression, followed by geostatistical modelling of residuals. The mean and 5<sup>th</sup> and 95<sup>th</sup> percentiles were produced as output datasets for each of the six depths. Viscarra Rossel et al. (2015) state that compared to the independent test set of sites reserved for validation, the SLGA AWC model explained only about 30% of the total variation in the test data and the proportion of the validation values (the coverage probability) that fell within the 90% confidence interval was between 0.87 and 0.84, decreasing with depth.

The units for the SLGA AWC dataset are percent, so they were converted to mm and constrained by depth using the SLGA DES dataset, to match the PTF outputs.

### **2.3. Pedotransfer Functions**

To test whether AWC can be modelled more precisely using PTFs and the more reliably predicted SLGA soil attributes as input parameters, multiple PTFs were used: a DUL (Lit DUL; Equation 1) and an LL15 (Lit LL15; Equation 2) from Littleboy (1997), and a DUL (Pad DUL; Equation 3) and two CLLs (Pad CLL1 and Pad CLL2; Equation 4 and Equation 5) from Padarian Campusano (2014):

$$DUL = 0.3486 - 0.0018 \textit{sand} + 0.0039 \textit{clay} + 0.0228 \textit{OC} - 0.0738 \textit{BD} \quad (1)$$

$$LL15 = 0.0854 - 0.0004 \textit{sand} + 0.0044 \textit{clay} + 0.0122 \textit{OC} - 0.0182 \textit{BD} \quad (2)$$

$$DUL = 0.2739 + 0.005033 \textit{clay} + 3.158 \times 10^{-5} \textit{sandCEC} - 1.96 \times 10^{-5} \textit{sand}^2 - 0.00256 \textit{clayBD} \quad (3)$$

$$CLL1 = 0.1476 + 9.002 \times 10^{-5} \textit{clay}^2 - 0.00115 \textit{sand} - 9.752 \times 10^{-7} \textit{clay}^3 \quad (4)$$

$$CLL2 = 0.6151 \textit{DUL} - 0.02192 \quad (5)$$

The Littleboy (1997) PTFs were based on laboratory measured DUL and LL (from -1/3 and -15 bar analyses). The Padarian Campusano (2014) PTFs used a subset of 806 soil profiles from the APSoil database that includes field measurements of DUL and CLL (Dagliesh et al. 2012). The three AWC predictions were calculated as Lit AWC (Lit DUL minus Lit LL15), Pad AWC1 (Pad DUL minus Pad CLL1) and Pad AWC2 (Pad DUL minus Pad CLL2).

## 2.4. Data Processing and Modelling

The input and comparison datasets from the SLGA match the *GlobalSoilMap* (<https://www.globalsoilmap.net/>) specifications for spatial resolution (3 arcsecond), grid alignment and six soil depth classes. All the datasets were clipped to the study area boundary and divided into tiles of 200 x 200 grid cells prior to parallel processing in a super computer environment. Except for the LHC sampling and correlation matrices, all code was written in Python (<http://www.python.org>). Layer thickness for each of the six soil depths was calculated in mm from the depth layer upper and lower bounds (e.g. 5 to 15 cm) and modified where needed by the SLGA DES dataset.

Correlation matrices were generated in R (R Core Team, 2017) for the different combinations of input datasets required by each of Equations 1 to 5, for each of the six depths. For example, the six Lit DUL correlation matrices included sand, clay, OC and BD, with values derived using data for the whole study area for each of the inputs.

Each of the six soil depth layers was modelled separately. For every grid cell in each depth layer, the following steps were used to calculate AWC from each of the 3 PTF combinations listed in section 2.3 (Lit AWC, Pad AWC1, Pad AWC2):

1. Standard deviation (SD) was calculated from the 5<sup>th</sup> and 95<sup>th</sup> percentiles for the input variables using Equation 6 (Malone et al. 2011):

$$\sigma_i = \frac{UPL_i - LPL_i}{2 \times z} \quad (6)$$

where  $\sigma_i$  is the variance associated with prediction  $i$ , UPL and LPL are the upper and lower prediction limits, and  $z$  is the  $z$ -value used for a confidence interval (CI) which in this case is 90% and  $z = 1.64$ . A normal distribution is assumed.

2. LHC sampling with a correlation matrix (from the *R pse* library; Chalom and Prado, 2014), using means, SDs and a correlation matrix as inputs, produced fifty realisations of each input variable. Fifty realisations were chosen following the work of Malone et al. (2015) who found that there was little difference in outcome when using more than 50 samples.
3. 50 DUL and LL15/CLL values were calculated from the 50 input variable realisations using the PTFs.
4. 50 AWC values were calculated from the DUL and LL15/CLL values, constrained by the layer thickness, with units of mm.
5. From the 50 AWC values, the mean, median, 5<sup>th</sup> and 95<sup>th</sup> percentiles, and SD were calculated and written to file as geotiffs.

The tiled outputs were merged to form a single raster of the study area for each of the six depths, and additionally the 0-5, 5-15, 15-30, 30-60 and 60-100 cm soil depth layers were used to calculate 0-1 m AWC. The mean, median, 5<sup>th</sup> and 95<sup>th</sup> percentile values were summed to produce the 0-1 m AWC prediction for each grid cell. This aggregation of depths assumes high correlation between layers – for example, the 95<sup>th</sup> percentile for the 0 – 1 m layer is the sum of the 95<sup>th</sup> percentiles for each contributing layer. If the layers were uncorrelated, the 95<sup>th</sup> percentile would end up closer to the mean. The SD for the 0-1 m AWC was calculated from the summed 5<sup>th</sup> and 95<sup>th</sup> percentiles, as per Equation 6.

The upper five SLGA AWC depth layers were also combined to create a 0-1 m dataset, with mean, 5<sup>th</sup> and 95<sup>th</sup> percentile values being summed for each grid cell. As for the PTF-derived AWCs, the SD for the 0-1 m AWC was calculated using Equation 6.

## 2.5. Uncertainty Comparison

In this paper we have used the 5<sup>th</sup> and 95<sup>th</sup> percentiles from the SLGA AWC and the 50 PTF-derived realisations of AWC (Lit AWC, Pad AWC1, Pad AWC2) as the LPL and UPL values when calculating a 90% prediction interval (PI). The 90% PI indicates that 90% of the variability of a modelled dataset falls within this range and is used here as a proxy for precision. A smaller value, i.e. when the 5<sup>th</sup> and 95<sup>th</sup> percentiles are closer together, represents less variability and more precision or confidence in the value of a grid cell. These predicted AWC datasets are not being compared with field calculated PAWC values; an assessment of the accuracy of these estimates, for example using prediction interval coverage probability (PICP; Shrestha and Solomatine, 2006; Malone et al. 2011), is the subject of future work.

90% PIs were calculated for the SLGA AWC, Lit AWC, Pad AWC1 and Pad AWC2 datasets, for the six *GlobalSoilMap* depths and 0-1 m by subtracting the 5<sup>th</sup> percentile value from the 95<sup>th</sup> percentile.

To compare the modelled AWC datasets, the SLGA AWC mean value, 90% PI and (for the 0-1 m) SD datasets were subtracted from the other three AWC predictions, averaged across the study area and then normalised by

the average thickness of the depth layer, giving units of mm of AWC per cm of soil. This was done for the six standard depths and 0-1 m to allow direct comparison of the results for each soil depth.

### 3. RESULTS

The averaged and normalised differences in the mean, 90% PI and SD values for the SLGA AWC and the PTF-derived AWCs are shown in Figure 2 for Lit AWC, in Figure 3 for the Pad AWC1 and in Figure 4 for the Pad AWC2. Negative values occur where the SLGA AWC has the larger mean, 90% PI or SD value compared to the PTF-derived AWC. Positive values indicate the reverse.

The general trend for all three PTF-derived AWC datasets is to predict smaller mean AWC values for the study area with greater precision than the SLGA AWC. That is, the average 90% PI is smaller for the PTF-derived AWC datasets compared to the SLGA AWC, indicating reduced variability, and this difference is consistent going down the soil profile to 1 m. This trend is quite marked for the Lit AWC and Pad AWC2 predictions (Figures 2 and 4), and less so for the Pad AWC1 prediction (Figure 3) where the bars showing one SD for the averaged 90% PI are much larger. To place the average differences in context, the mean, 90% PI and SD for the 0-1 m SLGA AWC predictions averaged over the study area are 1.33 mm/cm, 1.31 mm/cm and 0.40 mm/cm respectively.

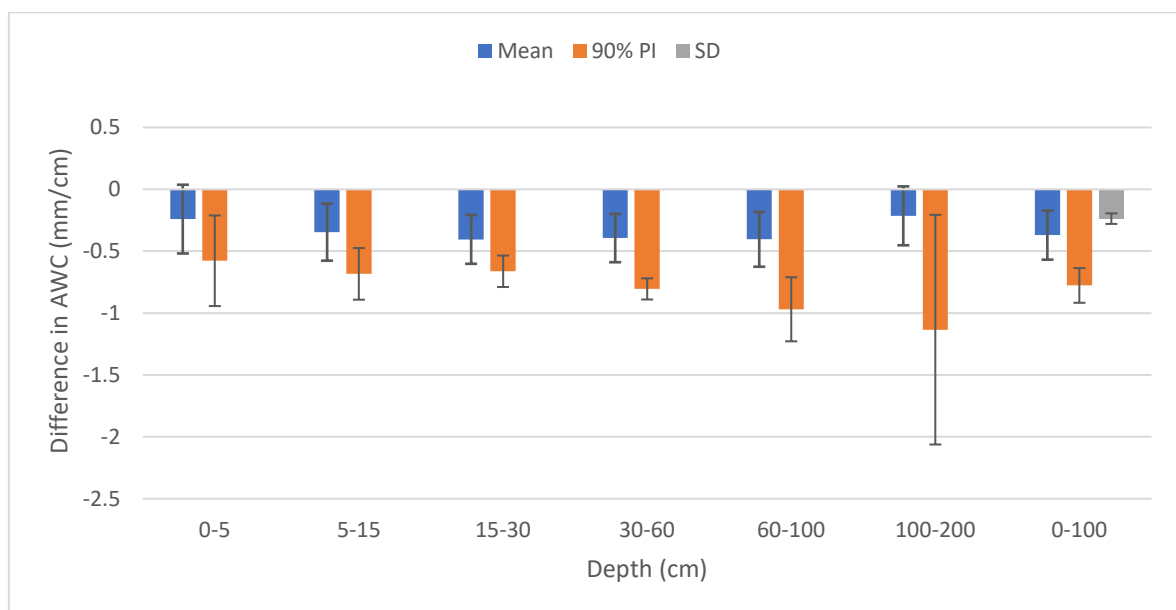


**Figure 2.** Differences in the mean, 90% PI and SD values for Lit AWC minus SLGA AWC averaged across the study area and normalized by average layer thickness for the six standard depth layers and 0-1 m. The error bars show +/- 1 standard deviation from the average difference. Negative numbers occur when the Lit AWC values are smaller than the SLGA AWC values.

In the 1-2 m depth layer the SLGA DES constraint affects approximately half the study area, resulting in no data in this depth range for most of the uplands along the Great Dividing Range and much of western NSW. The SLGA DES maximum depth in the study area is 1.76 m, with a mean thickness of 14 cm for the 1-2 m depth class. The reduced area with data at this depth contributes to the larger 90% PI error bars (+/- 1 SD of the average difference) for the 1-2 m depth compared to the other depths shown in Figures 2 to 4. There could also be bias in the types of soils which have depths greater than 1 m and/or bias in the input datasets, e.g. Viscarra Rossel et al. (2015) state that the predictor covariates are usually representative of surface processes.

The standard deviation bars shown on either side of the average mean, 90% CI and SD values indicate the variability in the differences between the predictions across the study area. The average mean, 90% CI and SD of Pad AWC1 differed the least from the SLGA AWC, but variability in the differences across the study area was noticeably higher.

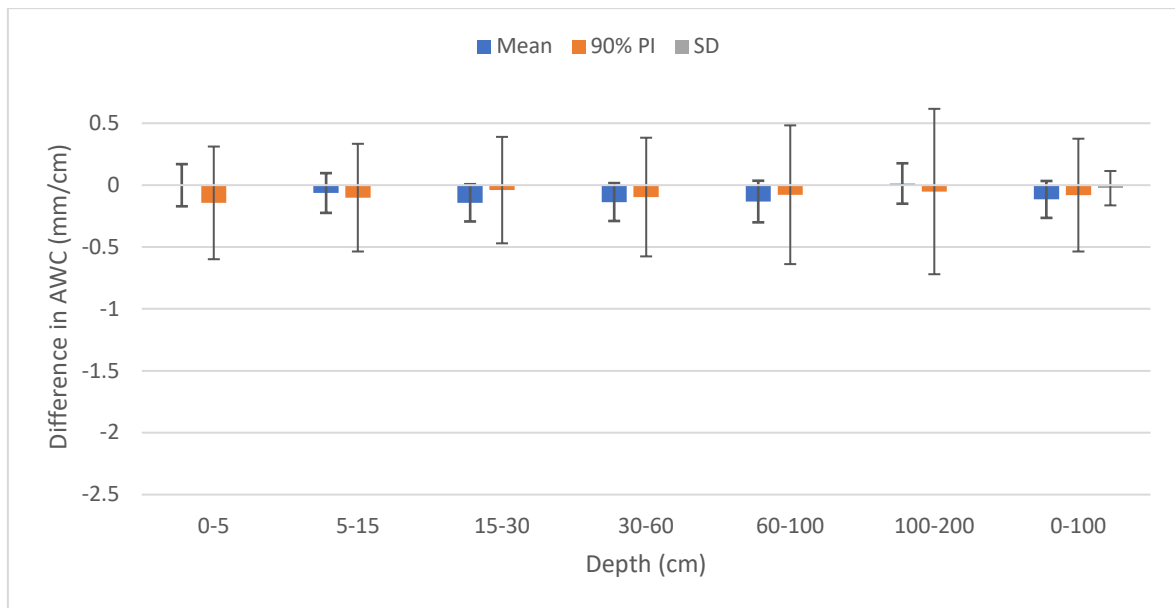


**Figure 3.** Differences in the mean, 90% PI and SD values for Pad AWC1 minus SLGA AWC, averaged across the study area and normalized by average layer thickness for the six standard depth layers and 0-1 m. The error bars show +/- 1 standard deviation from the average difference. Negative numbers occur when the Pad AWC1 values are smaller than the SLGA AWC values.

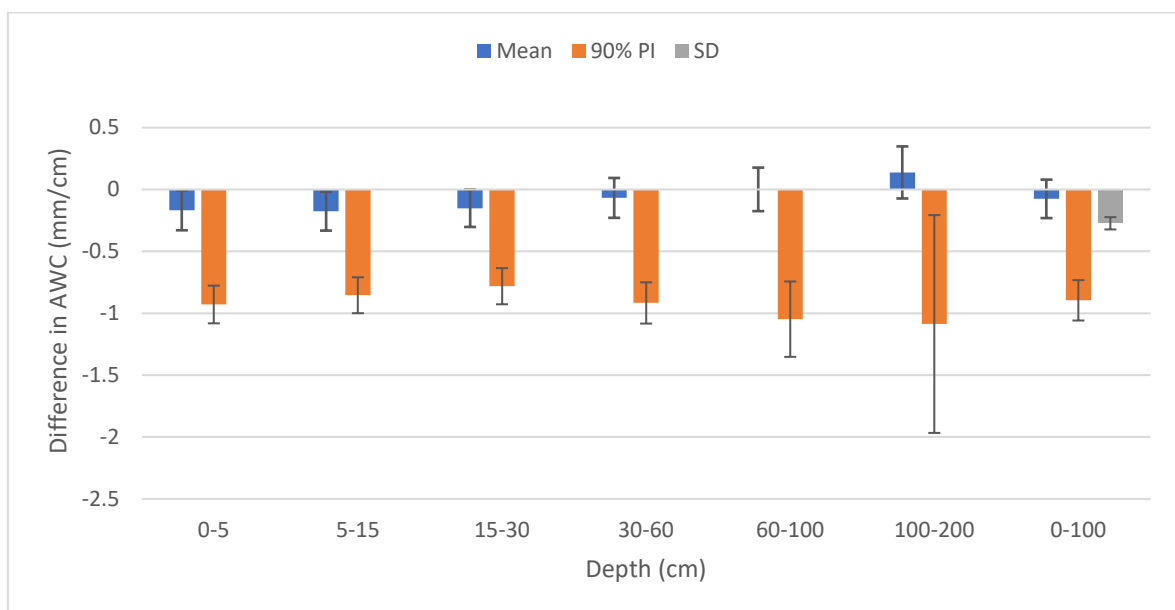


**Figure 4.** Differences in the mean, 90% PI and SD values for Pad AWC2 minus SLGA AWC, averaged across the study area and normalized by average layer thickness for the six standard depth layers and 0-1 m. The error bars show +/- 1 standard deviation from the average difference. Negative numbers occur when the Pad AWC2 values are smaller than the SLGA AWC values.

#### 4. DISCUSSION AND CONCLUSIONS

The SLGA AWC was modelled using more than 30 environmental layers (such as gamma radiometrics, elevation, NDVI, land cover, rainfall, air temperature) and depth-harmonised AWC derived from field site data (Viscarra Rossel et al. 2015). The PTF-derived AWC predictions presented here used the SLGA predictions of the easier-to-measure soil attributes such as clay, sand, BD, CEC and OC. The model validation statistics for these SLGA attributes for the 0-5 cm depth (e.g.  $R^2$  of 0.53, 0.49, 0.53, 0.79 and 0.66 respectively) were all better than those of the SLGA AWC ( $R^2$  of 0.29; Viscarra Rossel et al. 2015), indicating that the former are more reliable datasets. This was partly due to the small size of the field dataset available for the SLGA AWC prediction. The higher  $R^2$  values are likely to have contributed to the greater precision of the PTF-derived AWC predictions compared with those of the SLGA AWC.

Austin and Stockmann, Using pedotransfer functions to improve the precision of spatially predicted available water capacity

The mean AWC predictions across the study area for Lit AWC and Pad AWC2 are generally lower than the SLGA AWC, whereas the Pad AWC1 predictions were similar. This highlights the need for comparison with measured PAWC data to assess the accuracy of these predictions so that the best one can be chosen. It may be that accuracy and precision vary over the study area and the different predictions may represent some areas better than others. The differences in Pad AWC1 and Pad AWC2 result from independently modelling Pad DUL and Pad CLL1 to calculate Pad AWC1. This introduces a lot of variation in the summed Pad AWC1 output, as can be seen in the error bars in Figure 3, whilst producing the most similar average mean, 90% PI and SD when compared to the SLGA AWC. For Pad AWC2, Pad CLL2 is modelled directly from Pad DUL producing a prediction of AWC with lower 90% PI variability than the SLGA AWC across the study area. This has implications for the choice of PTF when modelling AWC.

Future work will include: exploring and incorporating the uncertainties associated with the PTFs, which has implications for both precision and accuracy; an assessment of whether different patterns of variability occur when accounting for soil texture, e.g. when clay is dominant; and to use PICP to evaluate the proportion of an observed dataset falling within the 90% PI and to give an indication of accuracy and reliability of the PTF-derived AWC.

## ACKNOWLEDGMENTS

This work was funded by the Grains Research and Development Corporation Project CSP00210 ‘Methods to predict plant available water capacity (PAWC)’ and the CSIRO. The authors would like to thank the following people for their advice: Ross Searle, Brendan Malone, Sanji Pallegedara Dewage and John Gallant of the CSIRO, and Jose Padarian of the University of Sydney, Australia.

## REFERENCES

- Bouma, J. (1989). Using Soil Survey Data for Quantitative Land Evaluation. *Advances in Soil Science*, 9, 177-213.
- Chalom, A. and Prado P. (2014). pse: parameter space exploration with Latin hypercubes. R package version 0.4.0. Available at <http://CRAN.R-project.org/package=pse>
- Dalglish, N.P., Cocks, B., and Horan, H. (2012). APSoil - providing soils information to consultants, farmers and researchers. 16th Australian Agronomy Conference, Armidale, NSW.
- Grundy, M.J., Viscarra Rossel, R.A., Searle, R.D., Wilson, P.L., Chen, C. and Gregory, L.J. (2015). Soil and Landscape Grid of Australia. *Soil Research*, 53, 835-844.
- Jenny, H. (1941). Factors of soil formation, a system of quantitative pedology. McGraw-Hill, New York.
- Littleboy, M. (1997). Spatial generalisation of biophysical simulation models for quantitative land evaluation: A case study for dryland wheat growing areas of Queensland. PhD. Brisbane, University of Queensland.
- Malone, B.P., McBratney, A.B. and Minasny, B. (2011). Empirical estimates of uncertainty for mapping continuous depth functions of soil attributes. *Geoderma*, 160 (3–4), 614-626
- Malone, B.P., Kidd, D.B., Minasny, B. and McBratney, A.B. (2015). Taking account of uncertainties in digital land suitability assessment. *PeerJ*, 3:e1366. <http://dx.doi.org/10.7717/peerj.1366>
- McBratney, A.B., Mendonça Santos, M.L. and Minasny, B. (2003). On digital soil mapping. *Geoderma*, 117, 3-52.
- Padarian Campusano, J.S. (2014). Provision of soil information for biophysical modelling. Masters Thesis. The University of Sydney. URL <http://hdl.handle.net/2123/12278>
- Pebesma, E.J. and Heuvelink, G.B.M. (1999). Latin hypercube sampling of gaussian random fields. *Technometrics* 41(4): 303-312. <http://dx.doi.org/10.1080/00401706.1999.10485930>
- R Core Team (2017). R: a language and environment for statistical computing. Vienna: R Foundation for Statistical Computing. Available at <http://www.R-project.org/>
- Shrestha, D.L. and Solomatine D.P. (2006). Machine learning approaches for estimation of prediction interval for the model output. *Neural Networks* 19: 225–235. <http://dx.doi.org/10.1016/j.neunet.2006.01.012>
- Verburg, K., Cocks, B., Manning, W., Truman, G., Schwenke, G. (2017). APSoil plant available water capacity (PAWC) characterisation of select Liverpool Plain soils and their landscape context. CSIRO, Canberra. <https://doi.org/10.25919/5bd204aac1892>
- Viscarra Rossel, R.A., Chen, C., Grundy, M.J., Searle, R.D., Clifford, D., Odgers, N., Holmes, K., Griffin, T., Liddicoat, C., Kidd, D. (2014). Soil and Landscape Grid National Soil Attribute Maps - Available Water Capacity (3" resolution) - Release 1. v5. CSIRO. Data Collection. <https://doi.org/10.4225/08/546ED604ADD8A>
- Viscarra Rossel, R.A., Chen, C., Grundy, M.J., Searle, R., Clifford, D. and Campbell, P.H. (2015). The Australian three-dimensional soil grid: Australia’s contribution to the *GlobalSoilMap* project. *Soil Research*, 53: 845-864.